First-principles interatomic potentials for transition-metal aluminides. III. Extension to ternary phase diagrams

Mike Widom and Ibrahim Al-Lehyani
Department of Physics, Carnegie Mellon University, Pittsburgh, Pennsylvania 15213

John A. Moriarty
Lawrence Livermore National Laboratory, University of California, Livermore, California 94551
(Received 20 January 2000)

Modeling structural and mechanical properties of intermetallic compounds and alloys requires detailed knowledge of their interatomic interactions. The first two papers of this series [Phys. Rev. B **56**, 7905 (1997); **58**, 8967 (1998)] derived first-principles interatomic potentials for transition-metal (TM) aluminides using generalized pseudopotential theory (GPT). Those papers focused on binary alloys of aluminum with first-row transition metals and assessed the ability of GPT potentials to reproduce and elucidate the alloy phase diagrams of Al-Co and Al-Ni. This paper addresses the phase diagrams of the binary alloy Al-Cu and the ternary systems Al-Co-Cu and Al-Co-Ni, using GPT pair potentials calculated in the limit of vanishing transition-metal concentration. Despite this highly simplifying approximation, we find rough agreement with the known low-temperature phase diagrams, up to 50% total TM concentration provided the Co fraction is below 25%. Full composition-dependent potentials and many-body interactions would be required to correct deficiencies at higher Co concentration. Outside this troublesome region, the experimentally determined stable and metastable phases all lie on or near the convex hull of a scatter plot of energy versus composition. We verify, qualitatively, reported solubility ranges extending binary alloys into the ternary diagram in both Al-Co-Cu and Al-Co-Ni. Finally, we reproduce previously conjectured transition-metal positions in the decagonal quasicrystal phase.

I. INTRODUCTION

Intermetallic alloys exhibit scientifically interesting and technologically important structures and properties. Their special mechanical, thermal, and chemical properties invite practical applications.[1,2] Their complicated and fascinating crystal[3] and quasicrystalline[4] structures are of fundamental scientific interest. Because cohesion and atomic interactions govern crystal structure and important mechanical properties such as elastic constants of solids, understanding the interactions among atoms within intermetallic compounds should deepen our understanding of their novel structures and properties.[5,6]

Investigating the interatomic interactions in intermetallic compounds is a considerable theoretical challenge. *Ab initio* electronic-structure methods applied to low-symmetry intermetallic structures[7,8] can become computationally very demanding, due to large unit cells with many inequivalent atomic sites and the likelihood of structural and chemical disorder. Quantum-mechanically-based interatomic potentials,[9–14] on the other hand, are well suited to complex or disordered structures. At the same time, the multiplicity of chemical species requires the calculation of numerous interaction potentials, which may be composition dependent. The presence of transition-metal (TM) components may require that angular-dependent many-body interactions be considered if the TM concentrations are sufficiently high. Further, the dissimilar electronic structure of simple metals compared with transition metals requires a mixed basis for electronic states containing plane waves for sp electrons and localized orbitals for TM d electrons to calculate such potentials from first principles.

Previous papers [henceforth referred to as paper I (Ref. 15) and paper II (Ref. 16)] extended the formalism of the first-principles generalized pseudopotential theory (GPT) for elemental interatomic potentials[10] to aluminum-rich $Al_{1-x}TM_x$ binary intermetallics, and studied their applicability to the systems Al-Co and Al-Ni in detail. This paper further extends the GPT approach to ternary intermetallic alloys, specifically Al-Co-Cu and Al-Co-Ni. Previously calculated ternary alloy potentials[11,12] have treated only simple metals, without d-electron interactions, and noble metals, with assumed completely filled d shells. The present paper is a treatment of interatomic potentials in ternary alloys containing transition metals with partially filled d bands.

Our goal in the present paper is to test the ability of the GPT interatomic pair potentials, calculated in the zero-TM-concentration limit, to reproduce the experimentally known aluminide ternary phase diagrams. Thus we examine the mechanical stability of known structures against atomic displacements, and we examine the thermodynamic stability against decomposition of an alloy into phases of differing composition. Requiring mechanical and thermodynamic stability of all known phases, and at least thermodynamic instability of a set of hypothetical structures, places stringent constraints on the interatomic interactions.

Our work focuses on the ternary system Al-Co-Cu with some brief comparisons made with Al-Co-Ni. There are several reasons for this choice. A primary motivating factor is the existence of stable decagonal quasicrystal phases in these compounds with reasonably well-understood atomic structure. Furthermore, Al-Co-Cu in particular has numerous stable phases in the ternary diagram [see Fig. 1(a)] with well-defined compositions that are well isolated in composition and distinct in structure from binary alloys. These ternary

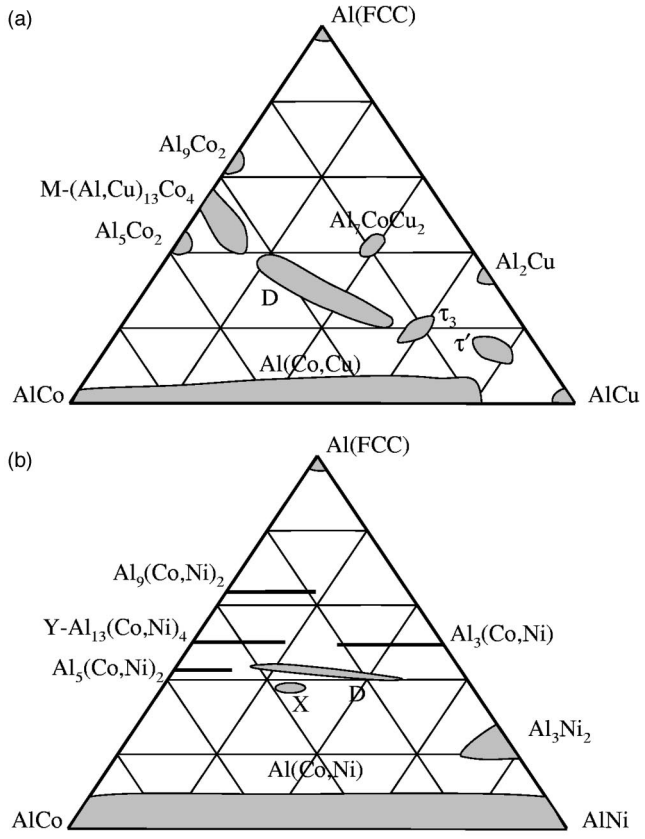

FIG. 1. Ternary phase diagrams of (a) Al-Co-Cu (adapted from Refs. 17 and 18) and (b) Al-Co-Ni (adapted from Ref. 19). Structural information is listed in Table I for all phases except for ''D'' (decagonal, Ref. 20) and ''X'' (unknown triclinic, Ref. 21)

phases appear at compositions where we may expect our potentials to apply with reasonable accuracy. Studying Al-Co-Cu gives us the chance to extend to the Al-Cu binary the degree of attention already devoted to Al-Co and Al-Ni. Finally, there will be interesting comparisons to make between the Al-Co-Cu and Al-Co-Ni potentials and phase diagrams. In Al-Co-Ni the composition fields of structures exhibit strong miscibility between Co and Ni [see Fig. 1(b)] in contrast to the behavior of Al-Co-Cu.

To test the ability of our potentials to reproduce the experimentally observed low-temperature phase diagram, we must demonstrate that the known low-temperature structures define the vertices of the convex hull of a scatter plot of cohesive energy versus composition. All other possible structures must lie above this convex hull. We cannot, of course, examine all conceivable structures, so we restrict our attention to structures that are either widely occurring simple structures or more complex structures observed in chemically similar compounds.

We find that our ternary potentials apply tolerably well within most regions of the $Al_{1-x-y}Co_xCu_y$ phase diagram of greatest interest. Along the the binary $Al_{1-y}Cu_y$ axis we find nearly perfect agreement with the known stable and metastable phase diagram up to $y=1/2$, using only the potentials evaluated at $y=0$. The only failure is the spurious appearance of the τ structures (described below in Sec. III) on the convex hull. Extending into the ternary $Al_{1-x-y}Co_xCu_y$ phase diagram, we find tolerable agreement provided $x+y<1/2$ and $x<1/4$. In this regime the only clear disagreement between our results and the known phase diagram is that the known stable structure Al_7CoCu_2 lies slightly (9 meV/atom) above the convex hull in our calculation. For $x \geqslant 1/4$ our ternary calculations fail because of known inadequacies of the binary $Al_{1-x}Co_x$ calculation at the present level of approximation.[16] Specifically, we do not adequately address the vacancy concentration in the O-$Al_{13}Co_4$ structure and we cannot treat Al_5Co_2 at the pair potential level. Encouragingly, the decagonal quasicrystal phase lies in a region of the phase diagram where our potentials may be expected to apply reasonably well.

The following section reviews the formalism and limitations of the generalized pseudopotential theory as applied in this paper. Section III applies the GPT potentials to calculate the binary alloy phase diagram of Al-Cu, followed by a treatment of ternary phase diagrams in Sec. IV. In Sec. V we discuss the utility of these potentials applied to decagonal quasicrystal structures, and we conclude in Sec. VI.

II. TOTAL-ENERGY CALCULATIONS

Paper I described the theoretical basis for calculating interatomic potentials in binary alloys within the generalized pseudopotential theory. Here, we review and extend some key ideas. For a general multicomponent alloy, the GPT interatomic potentials are explicit terms in a real-space expansion of total energy, which takes the form of a collective volume term, central-force pair interactions, and angular-force many-body interactions:

$$\begin{aligned} E_{\rm tot}(\mathbf{R}_1,\ldots,\mathbf{R}_N) = {} & NE_{\rm vol}(\Omega,\mathbf{c}) \\ & + \frac{1}{2}\sum_{\alpha,\beta}\sum_{i,j}{}' v_2^{\alpha\beta}(R_{ij};\Omega,\mathbf{c}) \\ & + \frac{1}{6}\sum_{\alpha,\beta,\gamma}\sum_{i,j,k}{}' v_3^{\alpha\beta\gamma}(R_{ij},R_{jk},R_{ki};\Omega,\mathbf{c}) \\ & + \frac{1}{24}\sum_{\alpha,\beta,\gamma,\delta}\sum_{i,j,k,l}{}' v_4^{\alpha\beta\gamma\delta} \\ & \times(R_{ij},R_{jk},R_{kl},R_{ik},R_{jl},R_{il};\Omega,\mathbf{c}) \\ & + \cdots. \end{aligned} \tag{1}$$

Here $\mathbf{R}_1,\ldots,\mathbf{R}_N$ denotes the positions of the N ionic cores and the prime on each sum over ion positions excludes all self-interaction terms. The quantity Ω is the average atomic volume in the alloy and $\mathbf{c}$ is a composition vector whose elements $x,y,\ldots$ depend upon the concentrations of the different chemical species. Indices $\alpha,\beta,\gamma,\delta,\ldots$ run over all chemical species, and indices $i,j,k,l,\ldots$ run over the individual ion sites occupied by the corresponding species.

The volume term $E_{\rm vol}(\Omega,\mathbf{c})$ is structure independent. It exerts no force on the individual atoms, but is important for determining the cohesive energy, equilibrium volume, and bulk modulus. The sums over the pair potentials ($v_2^{\alpha\beta}$) are the leading structure-dependent terms in the total energy. The many-body interactions ($v_3^{\alpha\beta\gamma}$ and $v_4^{\alpha\beta\gamma\delta}$) are presumed to be strongest among clusters of transition-metal atoms, due to the directional bonding of their d electrons, and weaker

among clusters containing simple-metal (e.g., aluminum) atoms. Consequently, the many-body interactions should be negligible at low TM concentrations, and grow progressively more important at higher TM concentrations. In pure elemental transition metals, the three- and four-body interactions are important, although higher-order interactions may often be neglected.[10,22] In general, both the pair and many-body potentials are long ranged with oscillatory tails arising from electron screening and/or sp-d hybridization. One can often demonstrate strong correlations between the oscillations of the potentials and favored or disfavored crystal structures.[5,6,15,16,23]

All terms in the GPT total-energy expansion depend on the atomic volume and chemical composition. Papers I and II discussed the detailed first-principles evaluation of full volume- and composition-dependent potentials for binary $Al_{1-x}TM_x$ alloys. The extension of those procedures to ternary systems is reasonably straigthforward, but it is clearly quite burdensome in practice when so many volumes and compositions are involved, as is the case here. For this reason, the discussion in the remainder of the paper uses only the GPT pair potentials evaluated in the limit of vanishing transition-metal concentration ($x=y=0$) and applied under the assumption of constant valence electron density, with the volume term treated as a constant. These simplifications are motivated by the observation[13] that the valence electron density varies slowly with x, near $x=0$, for $Al_{1-x}Co_x$ compounds. We have confirmed in paper II that the limiting $x=0$ potentials so applied achieve considerable success, although we did find that a few details in the alloy phase diagrams require the full volume- and composition-dependent GPT, and for $x>0.264$ many-body potentials as well. Nonetheless, the simplicity and elegance of the limiting aluminum-rich GPT treatment makes it the logical starting point for a consideration of ternary aluminide phase diagrams.

Calculated pair potentials for the Al-Co-Cu and Al-Co-Ni systems, computed in the zero-TM-concentration limit, are displayed in Fig. 2. Figure 2(a) shows interactions of Al atoms with themselves and with Cu, Ni, and Co. It is noteworthy that Al near-neighbor interactions (below about 3 Å) are strongly disfavored compared to interactions with transition metals such as Ni and Co. At low TM concentration this tends to favor structures with widely spaced transition-metal atoms, so as to maximize the number of Al-TM near neighbor bonds.

Figure 2(b) displays the pair interactions of the same transition-metal atoms. In the present work, we actually do not calculate the mixed transition-metal potentials $v_2^{\alpha\beta}$ with $\alpha\neq\beta$ explicitly. Rather, we make approximations based upon first-order expansions of the total energy in the atomic number difference $Z_\alpha - Z_\beta$. Thus the v_2^{CoNi} potential is set to the average $(v_2^{\mathrm{CoCo}}+v_2^{\mathrm{NiNi}})/2$, and for v_2^{CoCu} we simply employ v_2^{NiNi}. The plausibility of these approximations is supported by noting how close the Ni-Ni potential lies to the average of the Co-Co and Cu-Cu potentials. Quantitatively, the magnitude of $v_2^{\mathrm{NiNi}}-(v_2^{\mathrm{CoCo}}+v_2^{\mathrm{CuCu}})/2$ does not exceed 0.03 eV for $r\geq 2.5$ Å. One final point to note in Fig. 2(b) is the apparent strong binding of Co-Co pairs at unphysically short distances. This feature is a known difficulty of the unbalanced pair interactions for TM near neighbors. In reality the Co atoms repel at these distances due to contributions that enter the total energy only at the three- and four-body potential level in our expansion.

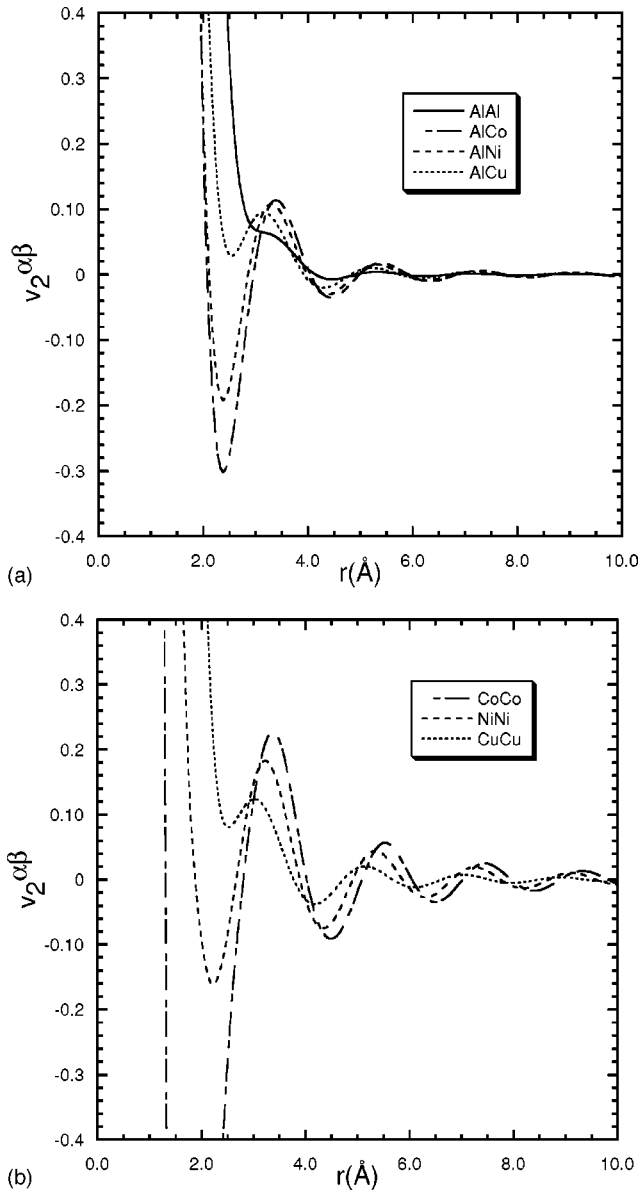

FIG. 2. Interatomic pair potentials calculated in the limit $x,y\rightarrow 0$. (a) Aluminum interactions. (b) Transition-metal interactions.

While we find tolerable qualitative agreement between our calculations and the experimentally determined phase diagrams, we do encounter certain difficulties that we believe can be traced back to the approximations employed. First of all, taking the limit of vanishing transition-metal concentration, and making the assumption of constant electron density, eliminates the variation of the volume term and pair potentials with composition and atomic volume. This causes small systematic errors in our calculated total energies and diminishes our ability to address vacancies and substitutional disorder over a composition range. Second, by dropping the many-body interactions we introduce significant errors in the energies of structures containing transition-metal near neighbors. We lose important angle-dependent effects, and we encounter difficulties with strong unbalanced transition-metal pair attractions.

TABLE I. Structural data for real and hypothetical Al-Cu phases up to $y=0.5$.

Name	Pearson symbol (Strukturebericht)	Space group	Reference	y
fcc	$cF4$ $(A1)$	$Fm\bar{3}m$	29	0.0000
hcp	$hP2$ $(A3)$	$P6_3/mmc$	29	0.0000
bcc	$cI2$ $(A2)$	$Im3m$	29	0.0000
$Al_{12}W$	$cI26$	$Im3$	29	0.0769
Al_6Mn	$oC28$ $(D2_h)$	$Cmcm$	29	0.1429
Al_9Co_2	$mP22$	$P2_1/a$	29	0.1818
O-$Al_{13}Co_4$	$oP102$	$Pmn2_1$	24	0.2353
$Al_{75}Co_{22}Ni_3$	$mC34$-1.8	$C2/m$	30	0.2500
W_3O	$cP8$ $(A15)$	$Pm3n$	29	0.2500
$AuCu_3$	$cP4$ $(L1_2)$	$Pm3m$	29	0.2500
Fe_3Al	$cF16$ $(D0_3)$	$Fm3m$	29	0.2500
Al_3Ti	$tI8$ $(D0_{22})$	$I4/mmm$	29	0.2500
Al_3Ni	$oP16$ $(D0_{11})$	$Pnma$	29	0.2500
M-$Al_{13}Co_4$	$mC102$	$C2/m$	25,29	0.2637
Al_5Co_2	$hP28$	$P6_3/mmc$	29	0.2857
Al_5Fe_2	$oC16$	$Cmcm$	29	0.2857
Al_7CoCu_2	$tP40$	$P4/mnc$	29	0.3000
Al_2Cu	$tI12$ $(C16)$	$I4/mcm$	29	0.3333
Al_7Cu_4Li	$cF12$	$Fm\bar{3}m$	29	0.3333
Al_4CoLa	$oP12$	$Pmma$	29	0.3333
τ_3 (Al_3Cu_2)	$hP5$ $(D5_{13})$	$P\bar{3}m1$	29	0.4000
τ_n			31	0.375–0.400
Al_4CoNi_2	cI112	$Ia\bar{3}d$	29	0.4286
CsCl	$cP2$ $(B2)$	$Pm3m$	29	0.5000
NaCl	$cF8$ $(BA4)$	$Fm3m$	29	0.5000
AuCu	$tP4$ $(L1_0)$	$P4/mmm$	29	0.5000
AlCu (HT)	$oC16$	$Cmmm$	28	0.5000
AlCu (LT)	$mC20$	$C2/m$	27,29	0.5000

These difficulties are illustrated in our findings reported in paper II. There we found that we could reproduce the known phase diagram for $Al_{1-x}Co_x$ up to $x=0.264$ using only GPT pair potentials calculated in the $x=0$ limit. However, the orthorhombic and monoclinic variants of $Al_{13}Co_4$ appeared with substantially higher vacancy concentrations than the latest experimental assessments[24,25] place them. Consideration of volume- and composition-dependent potentials should resolve these difficulties. Furthermore, at $x=0.2857$, the pair potentials favored Al_5Fe_2 over the true structure of Al_5Co_2. Inclusion of three- and four-body TM interactions resolved this problem. In the case of Al-Ni we found, using the $x=0$ potentials, that the Al_9Co_2 structure incorrectly falls on the convex hull, and that $Al_{13}Co_4$ preempts the $D0_{11}$ structure of Al_3Ni. Both of these difficulties were alleviated by use of the volume- and composition-dependent potentials.

III. Al-Cu BINARY PHASE DIAGRAM

Since Cu is a noble metal, with a completely filled *d* shell in the atom and nearly filled *d* bands in the elemental metal, its many-body interactions are relatively weak compared with those among other transition-metal atoms. That suggests that the GPT might apply to the compound $Al_{1-y}Cu_y$ for all y from 0 to 1, keeping only the volume term and the pair interactions. For our present purposes, however, we will focus on the Al-rich side, up to $y=1/2$, because this is the concentration range that interests us in the present work and because we employ pair potentials calculated in the limit of vanishing Cu concentration. In this limit, Cu has a calculated *sp* valence of 1.805, compared to a value of 1.651 in the elemental metal and a value of 1.0 in the free atom.

The aluminum-rich side of the $Al_{1-y}Cu_y$ phase diagram[26] is very sparse. Between pure fcc aluminum at $y=0$ and AlCu at $y=1/2$ there exists only one stable phase, Al_2Cu at $y=1/3$. In contrast, the copper-rich side contains a large number of phases, many with both low- and high-temperature variants, and many with complex or unknown structure. Even AlCu, at $y=1/2$, has both a complicated low-temperature (LT) structure[27] $mC20$ and a high-temperature (HT) variant, either $oP16$ or $oC16$ of unspecified structure.[28] Both variants of AlCu are considered to be vacancy-ordered phases based upon the $B2$ (CsCl) structure.

Table I lists the structures considered in our evaluation of the Al-Cu binary potentials. Most of these structures are self-explanatory. For example, Cu replaces the transition metal in Al-TM compounds. In other cases the assignment of Al and Cu atoms among the sites may be deduced from the overall stoichiometry. Certain structures require specific comment because of choices made about their composition or because

their structures are unfamiliar. The orthorhombic phase O-$Al_{13}Co_4$ is taken to be fully occupied.[24] We incorporate vacancies in $Al_{75}Co_{22}Ni_3$ by removing one Al from each pair with separation less than 2.4 Å as discussed in paper II. The monoclinic phase M-$Al_{13}Co_4$ incorporates vacancies as proposed by Hudd and Taylor.[32] However, its extension to the ternary M-$(Al,Cu)_{13}Co_4$ utilizes the fully occupied structure.[25]

An interesting family of vacancy-ordered phases are the so-called τ phases[33] that occur as metastable phases in binary Al-Cu (Ref. 34) and as metastable or stable phases in Al-Ni (Ref. 31) and in ternary systems such as Al-Cu-Ni (Ref. 33) and Al-Co-Cu (Ref. 35). These structures are based upon the $B2$ structure, with compositional modulation along the [111] direction. In the $B2$ structure of Al-TM alloys the (111) planes are occupied, alternately, by Al or by TM atoms. The compositional modulation deletes certain TM planes, with the pattern of occupied (O) or vacant (V) TM planes following a ''Fibonacci'' sequence.[31] For example, in the τ_3 structure every third TM layer is vacant in the pattern OVO. This is the structure of the stable phase Al_3Ni_2 and the metastable phase Al_3Cu_2. The τ_5 structure is the pattern $OVOVO$, τ_8 is formed by joining a single repeat unit of τ_3 to a single repeat unit of τ_5, and τ_{13} joins τ_5 with τ_8.

Because the structure of the HT phase at composition $y=1/2$ is unknown, we created a test structure consistent with the known lattice constants and symmetries. Thus we start with a $B2$ structure with lattice constant a_0. The unit cell of our HT contains 18 unit cells of the $B2$ structure and has lattice constants $(\sqrt{2},3\sqrt{2},3)$ in units of a_0. We introduce a pair of Al vacancies into one layer perpendicular to the c axis and a pair of Cu vacancies into a layer $c/2$ away. The choice of vacant sites is made consistently with C-face centering, producing an $oC16$ structure.

For each of the structures listed in Table I we isotropically scaled the lattice constants so that the free-electron density matched that of pure fcc aluminum (0.180 76 $Å^{-3}$). We employ a free-electron valence of 3 for each Al atom and 1.805 for each Cu atom.[15] The structures were then relaxed until the average force per atom dropped below 10^{-3} eV/Å; then their total energy is reported. Figure 3 shows a scatter plot of the data. We classify the stability of structures according to their displacements upon relaxation and display this information using plotting symbols. Highly symmetric structures do not relax because forces balance exactly. Certain structures had displacements beyond 0.3 Å/atom. We consider those structures to be unstable and display the unrelaxed energies of these structures. To remove a strong linear slope of the energy vs composition data, we subtract all energies from the tie-line joining fcc aluminum to Al_3Cu in the $L1_2$ structure, defining ΔE.

Inspection of Fig. 3 reveals that the convex hull is well respected. Up to $y=0.5$ there is only a single unreported structure, the τ_5 structure at $y=0.375$, which touches the convex hull. The metastable τ_3 structure of Al_3Cu_2, and the high-temperature variant of AlCu both lie slightly above the convex hull, consistent with their near stability. Similarly, Al_7Cu_4Li, with an Al atom replacing Li, nearly touches the convex hull. Extending into the AlCuLi ternary diagram could possibly stabilize this structure. Both Al_9Co_2 and $D0_{11}$

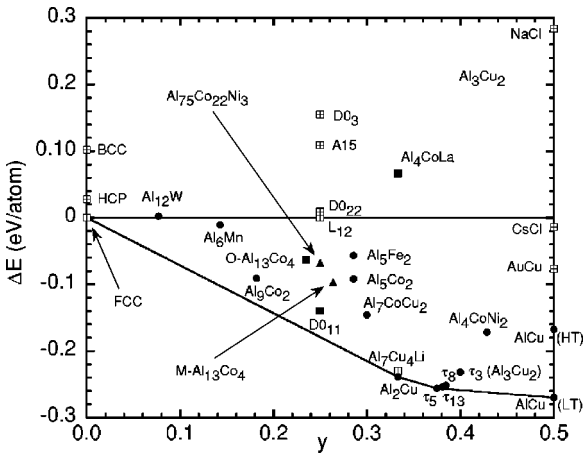

FIG. 3. Scatter plot of binary $Al_{1-y}Cu_y$ structural energies $\Delta E(y)$. Plotting symbols indicate displacements under relaxation: unrelaxed symmetric structure (⊞), $\Delta R \leqslant 0.1$ Å (●); 0.1 Å $< \Delta R \leqslant 0.2$ Å (▲), 0.2 Å $< \Delta R \leqslant 0.3$ Å (■), and unrelaxed unstable structure (□). The solid line indicates the convex hull.

(the structure of Al_3Ni) lie above, but close to, the convex hull as is appropriate considering the proximity of Co and Ni to Cu in the periodic table.

IV. TERNARY PHASE DIAGRAMS

Ternary phase diagrams for both Al-Co-Ni and Al-Co-Cu are known in some detail.[19,17] The labeled regions in Fig. 1 represent the known stable phases. Al-Co-Cu [Fig. 1(a)] exhibits several distinct structures within well-separated composition fields.[17] The ternary compounds include Al_7CoCu_2 (a tP40 structure containing cubes of Al centered with Cu atoms[36]), the decagonal phase,[20] and a pair of phases (τ_3 and τ') believed to be related to the vacancy-stabilized phases described above in the context of binary Al-Cu structures. At 50% Al concentration, the $B2$ (CsCl) structure of Al(Cu,Co) extends from AlCo nearly to AlCu. It is believed that vacancies proliferate within the ternary $B2$ structure.[37] The actual AlCu structure, as noted above, is a vacancy ordered $B2$ structure.

It is intriguing that the M-$(Al,Cu)_{13}Co_4$ phase (well known as a decagonal quasicrystal approximant), the decagonal phase composition field, the τ phases, and the vacancy-stabilized AlCu phase are nearly colinear in this phase diagram, lying near the line $2x+y=1/2$ connecting Al_3Co with AlCu. Along this line Cu substitutes for both Al and Co in equal numbers. This effect motivated construction of successful ''mock ternary'' Al-Co-Cu potentials[38] that started with binary Al-Co potentials[13] and then defined the interactions of Cu atoms as if Cu was a linear superposition of Al and Co. Remarkably, Raynor's[39] effective valences of $1+$ for Cu and $1-$ for Co yield a constant electron per atom ratio of 2 along this line, suggesting a possible link between this electron to atom ratio and formation of the quasicrystal phase.[40]

The phase diagram[19] of Al-Co-Ni [Fig. 1(b)] contrasts strongly[18] with Al-Co-Cu. Instead of well-isolated composition fields, the phase diagram of Al-Co-Ni is marked by highly elongated composition fields, with Ni and Co substituting for each other, but not replacing Al. The miscibility of

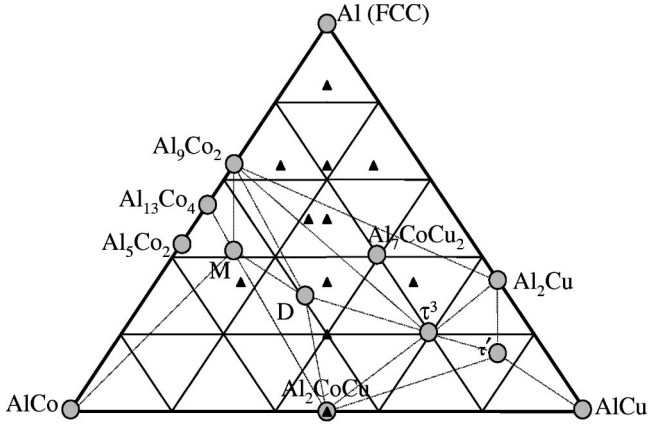

FIG. 4. Al-Co-Cu ternary phase diagram. Labeled circles denote experimentally observed phases. Triangles denote other compositions considered. Dashed lines border facets of convex hull in calculated $\Delta E(x,y)$.

Co and Ni in the $B2$ structure is complete. Many other binary structures extend far across the ternary diagram.

We begin our exploration of the ternary phase diagram with the compound Al-Co-Cu. Figure 4 reproduces the known ternary diagram and superposes some information about our calculations. Table II lists ternary structures representative of various points in the composition plane. The labeled circles in Fig. 4 represent the experimentally known structures we examined. The black triangles locate compositions at which we tested hypothetical structures. The dashed tie-lines define the edges of our calculated convex hull.

In some cases, where a real or hypothetical structure is not fully known, we made reasonable guesses. For example, we employed the Cockayne-Widom[38] model for the decagonal phase (denoted ''D'' in Fig. 4). A quasicrystal has no unit cell, so we actually studied a crystalline approximant with unit cell dimensions $60\times51\times4$ Å^3 of composition $Al_{586}Co_{178}Cu_{142}$. The fully occupied M-$(Al,Cu)_{13}Co_4$ structure (denoted ''M'' in Fig. 4) is taken from Freiburg and Grushko[41] in which Cu positions are specified. The ternary τ_3 phase is based upon the τ_3 structure of Al_3Cu_2, with the unit cell doubled along the three-fold axis. A single Cu atom is then replaced with a Co atom to create Al_6CoCu_3. The ternary τ' structure is based upon the τ_{13} unit cell, taking composition $Al_{36}Co_3Cu_{24}$ which is close to the experimentally reported composition. A simulated annealing procedure[16] established the optimal sequence of Al, Co, and Cu layers holding the atomic sites fixed at their ideal positions. Near-neighbor Co atoms were prohibited during the annealing in order to avoid overbinding at short distances.

TABLE II. Structural data for hypothetical Al-Co-Cu phases up to $x+y=0.5$.

Name	Pearson symbol	Space group	(x,y)
$Al_{12}(Cr,Mn)$	$cI26$	$Im\bar{3}$	(0.0385,0.0385)
$Al_{11}CoMo_4$	$tI8$	$I4/mmm$	(0.0625,0.1875)
			(0.1875,0.0625)
$Al_{11}CoMo_4$	$tI8$	$I4/mmm$	(0.0625,0.1875)
			(0.1875,0.0625)
Al_6MoNb	$tI8$	$I4/mmm$	(0.1250,0.1250)
$Al_{23}CuFe_4$	$cO28$	$Cmc2_1$	(0.1429,0.1071)
Al_4CoLa	$oP12$	$Pmma$	(0.1667,0.1667)
Al_4NiY	$oC24$	$Cmcm$	(0.1667,0.1667)
Al_8La_3Sc	$cF24$	$Fd\bar{3}m$	(0.2500,0.0833)
			(0.0833,0.2500)
Al_4LaY	$cF24$	$Fd\bar{3}m$	(0.1667,0.1667)
Al_8NiTi_3	$cP4$	$Pm\bar{3}m$	(0.2500,0.0833)
			(0.0833,0.2500)
Al_5CuHf_2	$cP4$	$Pm\bar{3}m$	(0.1250,0.2500)
			(0.2500,0.1250)
Al_3CuHo	$oI10$	$Immm$	(0.2000,0.2000)
Al_2FeNi	$cP2$	$Pm\bar{3}m$	(0.2500,0.2500)
Al_2HfZn	$cP4$	$Pm\bar{3}m$	(0.2500,0.2500)
Al_2NiY	$oC16$	$Cmcm$	(0.2500,0.2500)
Al_2CoY	$oC16$	$Cmcm$	(0.2500,0.2500)

A pictorial summary of our quantitative results is achieved by plotting total energies along special lines in the diagram. The special lines we choose are (a) $x=y$ (see Fig. 5), (b) $x+y=1/4$ (see Fig. 6) (c) $x+y=1/3$ (see Fig. 7) because many simple and well-known structures lie on these lines. Data point symbols are as in the corresponding figure for binary Al-Cu except for the addition of + symbols marking the convex hull and $\times$ symbols marking the intersections of our special lines with tie-lines between the two structures named adjacent to the marker. When one of these tie-lines meets the convex hull, the + and $\times$ symbols overlay each other.

For the most part, our calculated energies are consistent with the experimentally known phase diagram. The hypothetical structures lie above the convex hull, so that only known structures (or tie-lines joining them) lie on the hull. We now focus on a few points of discrepancy between our data and the experimental phase diagram. These points of disagreement indicate the limits of reliability of the GPT energies truncated at the pair-potential level and neglecting composition and volume dependence.

An immediately apparent problem is that no edge (dashed line) of the convex hull in Fig. 4 joins the experimentally known Al_7CoCu_2 structure, and thus that structure does not occupy a vertex of the convex hull. Indeed, the calculated energy of this structure lies 0.009 eV/atom above the convex hull. Likewise, no convex hull edge joins Al_5Co_2. This was expected from our prior discussion in Sec. II and reflects the need to include many-body interactions.

These same difficulties are evident in our quantitative plots of energy versus composition along special lines in Figs. 5–7. As noted above, Al_7CoCu_2 lies slightly above the convex hull, and thus tie-lines connecting to it (see $\times$ symbols) lie slightly above the hull. Along the lines $x+y=1/4$ and $x+y=1/3$ we expect difficulty near $y=0$ due to the known inadequacy of $x=0$ pair potentials for $Al_{1-x}Co_x$ at large x. For reference, we have placed the calculated energies of some binary structures on the energy diagram for $x+y=1/4$ at $y=0$. These fall below the convex hull of the energies for the structures we considered when calculating the ternary compounds. We did not consider these binaries as part of our ternary study because at this composition a more careful treateent of vacancy formation is needed. At $y=0$ on

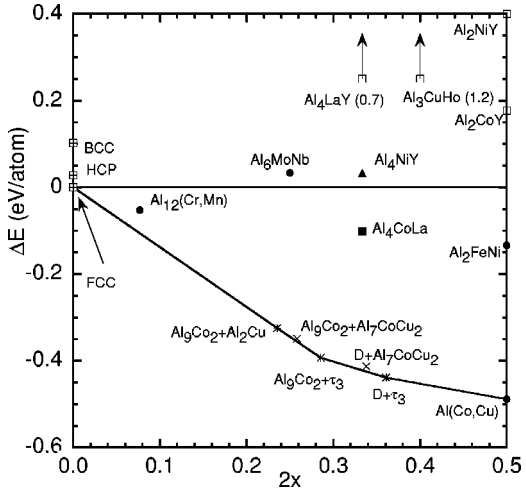

FIG. 5. Scatter plot of ternary structural energies $\Delta E(x,y)$ along the line $x=y$. Plotting symbols as in Fig. 3.

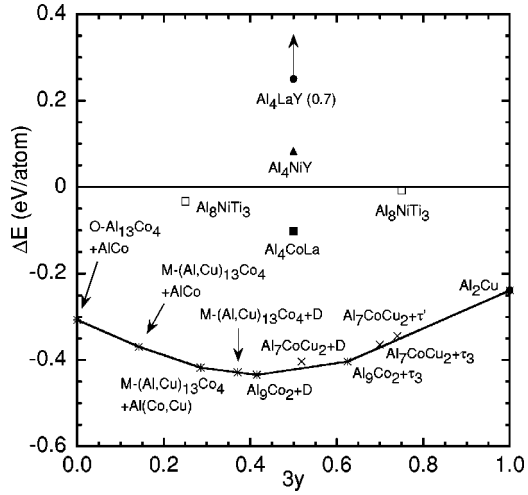

FIG. 7. Scatter plot of ternary structural energies $\Delta E(x,y)$ along the line $x+y=1/3$. Plotting symbols as in Fig. 3.

the line $x+y=1/3$ (see Fig. 7) the difficulty is that AlCo coexists with O-$Al_{13}Co_4$ rather than with Al_5Co_2.

Composition ranges

The ability of interatomic potentials to reproduce trends among distinct compounds is a further test of their applicability. We examined two special lines in the Al-Co-Ni phase diagram and contrasted them with the same lines in the Al-Co-Cu diagram. Our goal is to understand the differing abilities of transition metals to substitute for each other.

Along $x+y=0.1818$ we study the stability of the Al_9Co_2 structure as Cu or Ni replaces Co. As soon as we replace one out of the four Co atoms with Cu the energy rises above the convex hull. This is consistent with the experimental phase diagram [Fig. 1(a)] in which Cu is insoluble in Al_9Co_2. In contrast, we can replace any number of Co atoms with Ni and the structure remains on the convex hull. Thus our calculation shows the solubility of Ni in Al_9Co_2 extending over the entire line $x+y=0.1818$. In reality [see Fig. 1(b)], stability of $Al_9(Co,Ni)_2$ terminates after about half of the Co are replaced with Ni. It is likely that in a full GPT treatment including the atomic volume and composition dependence of the potentials this feature would be accurately captured, because it is known that the Al_9Co_2 structure lies slightly above the convex hull of the $Al_{1-y}Ni_y$ binary alloy when the full GPT potentials are employed. The trend of greater Ni solubility than Cu in Al_9Co_2 is faithfully reproduced.

Along $x+y=1/4$ we study the ability of Co to replace Ni in the $D0_{11}$ structure of Al_3Ni. We find that Co can fully replace Ni within this structure. Experimentally, up to half the Ni can be so replaced before a competing phase O-$Al_{13}(Co,Ni)_4$ appears. According to our calculations, and consistently with experiment, the same $D0_{11}$ structure is not stable for Al_3Cu; nor is it stable with limited amounts of Co replacing Cu. Again, the ability of Co and Ni to replace each other within their binary structures is faithfully reproduced, as is the relative inability of Co and Cu to replace each other in the same structures.

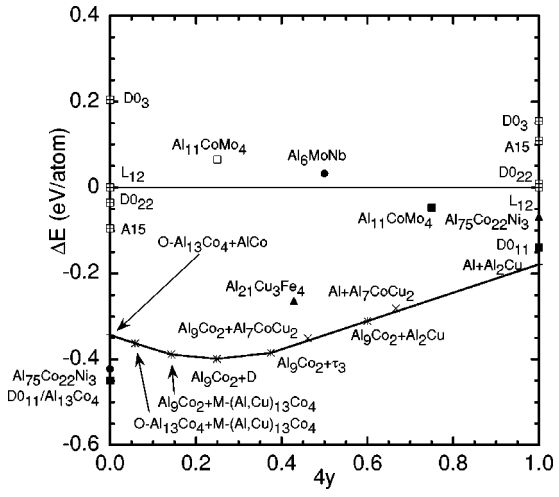

FIG. 6. Scatter plot of ternary structural energies $\Delta E(x,y)$ along the line $x+y=1/4$. Plotting symbols as in Fig. 3.

V. QUASICRYSTAL

The hope to model quasicrystal structures motivated the development of these ternary GPT potentials. We calculated the stability and cohesive energy of the decagonal quasicrystal phase in Al-Co-Cu. As a structural model for this phase we employ the model of Cockayne and Widom (CW).[38] This model was deduced from Monte Carlo simulations of the alloy using a nonrigorous total energy calculation based upon ''mock ternary'' interactions. Fortunately, in this structure there are no near-neighbor Co atoms. Thus, the Co-Co overbinding at short distances will not be problematic and we may directly apply the GPT potentials. Note that this model is one of many competing decagonal phase models (see Ref. 8 and references therein). We do not attempt to distinguish among competing models in the present paper because a more thorough treatment of transition-metal binding would be required than is possible within our present approximations.

According to our present calculations, this model quasicrystal enjoys both modest mechanical and thermodynamic stability. The median atomic displacement of 0.14 Å and mean atomic displacement of 0.18 Å is encouraging. How-

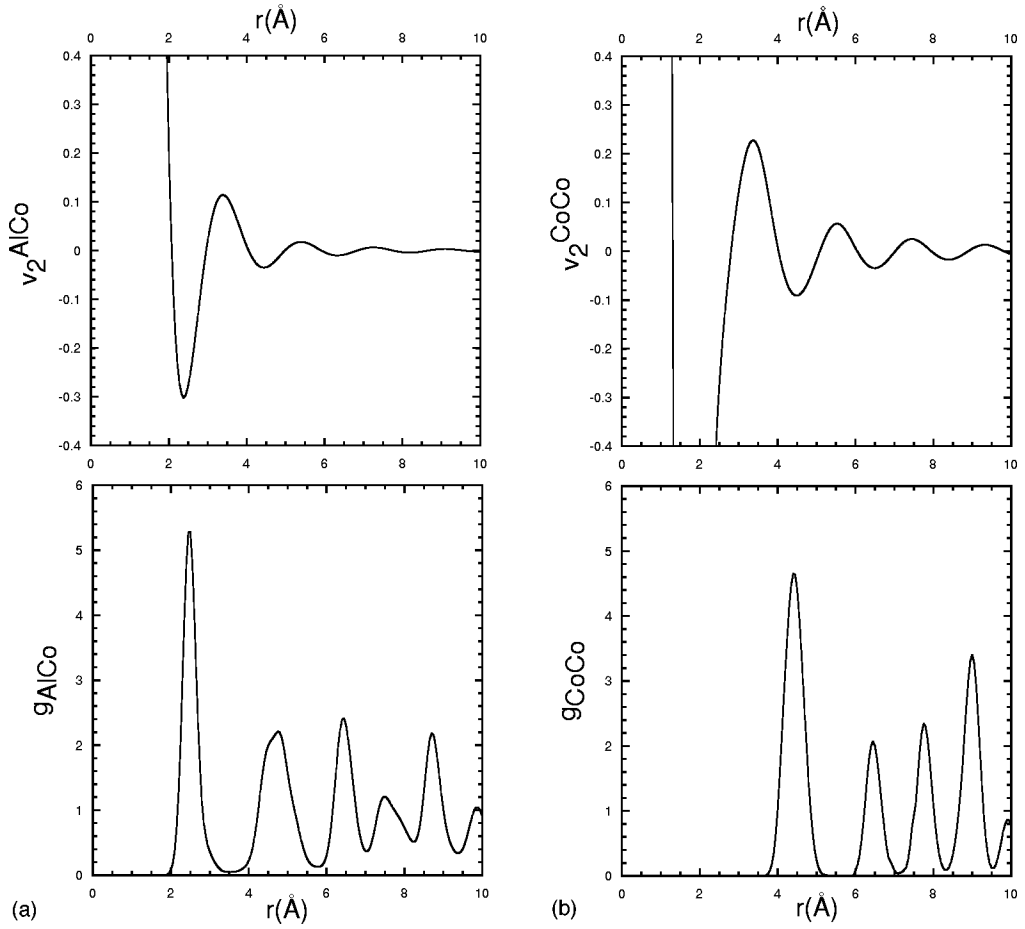

FIG. 8. Cobalt correlation functions in the decagonal phase of Al-Co-Cu exhibit maxima near minima of the pair potentials. (a) Al-Al potential and correlation function. (b) Co-Co potential and correlation function.

ever, a few Al atoms displace by over 1 Å. Such behavior has been found previously in Refs. 38,42,43. We attribute these large displacements to nearly flat potential energy surfaces around certain atomic positions that allow small errors in the forces to cause large atomic displacements. The thermodynamic stability of the decagonal phase is also limited. The quasicrystal phase lies only 37 meV/atom below the tie-line with τ_3, M-$(Al,Cu)_{13}Co_4$, and Al_2CoCu. A more exhaustive consideration of hypothetical structures, including other quasicrystal approximants and other crystalline structures, could possibly find structures that compete in energy with the quasicrystal.

Favorable bond lengths contribute to the low energy of our quasicrystal model. Pair correlation functions $g_{\alpha\beta}(r)$ between atomic species α and β generally exhibit maxima near to separations r at which the potential $v_2^{\alpha\beta}(r)$ exhibits minima and vice versa. This relationship is especially notable for Al-Co and Co-Co pairs, as illustrated Fig. 8. The correlation functions in this figure incorporate Gaussian broadening to mimic the effects of thermal fluctuations at $T=1000$ K. Without broadening the correlation functions would be a dense collection of closely spaced δ functions.

All of the Al-Co near neighbors separations lie within the first deep minimum of the Al-Co pair potential around 2.4 Å. The second pair potential minimum at 4.4 Å and the third minimum at 6.4 Å likewise encompass strong second and third peaks of the pair correlation functions. The first minimum of the Co-Co pair potential occurs at an unphysically short separation. Fortunately, the CW model includes no Co-Co pairs with separations below 4 Å. However, the strong second and third Co-Co pair-potential minima, at 4.5 Å and 6.5 Å, respectively, match the first two peaks of the Co-Co pair correlation function.

A side effect of the favorable bonding environments of Co atoms is the existence of a highly stable Co network within the decagonal phase model. When the mean atomic displacement under relaxation is broken down according to atomic species we find mean displacements of 0.22 Å for Al atoms, 0.15 Å for Cu atoms, and 0.08 Å for Co atoms. Figure 9 illustrates a portion of a decagonal Al-Co-Cu structure and highlights the strong Co-Co bonds. In addition to the bonds drawn, there are favorable Al-Co and Co-Cu near-neighbor separations, as well as favorable farther neighbor separations. The bonds illustrated in Fig. 9 form edges of a pentagon-rectangle-triangle tiling, a well-known motif in decagonal quasicrystals and approximants. It is evident that the geometry of the decagonal phase structure exploits the oscillations of the interatomic pair potentials to achieve a low energy.

We are currently engaged in *ab initio* electronic-structure calculations of total energies in small-unit-cell Al-Co-Cu (Ref. 44) and Al-Co-Ni (Ref. 45) quasicrystal approximants. The information thus obtained will allow us to modify the TM interactions at short distances, formally including many-

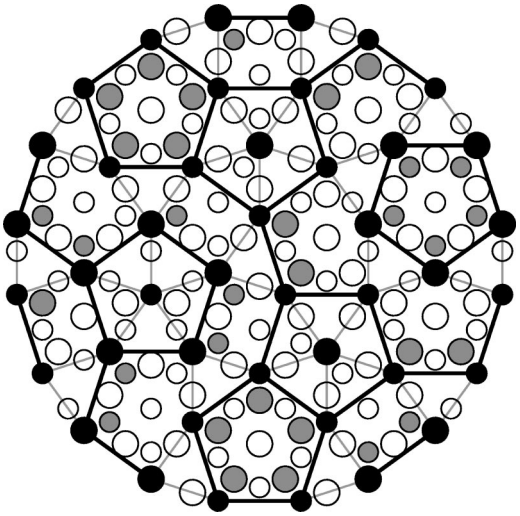

FIG. 9. Structure of the Al-Co-Cu decagonal phase. Open circles indicate Al atoms, gray disks Cu atoms, and black disks Co atoms. Large and small atoms occur in parallel layers 2 Å apart. Gray and black bonds joining neighboring Co atoms are 4.5 and 4.7 Å, respectively.

body interactions within the TM pair potentials.[46] The resulting pair interactions become structure dependent because they are tuned for atomic environments typical of the quasicrystal. They should allow modeling of the quasicrystal phase at the pair-potential level. Indeed, the structure displayed in Fig. 9 results from a Monte Carlo simulation[47] that takes sites characteristic of the Cockayne-Widom decagonal phase model and anneals the chemical occupation of those sites using modified GPT potentials. The structures that result are in close agreement with the predictions of Cockayne and Widom based upon mock ternary potentials.

VI. CONCLUSIONS

We have extended the generalized pseudopotential theory of interatomic potentials in binary transition-metal aluminides to ternary systems, and have developed first-principles pair potentials in the aluminum-rich limit for Al-Co-Cu and Al-Co-Ni alloys. The pair potentials reproduce many features of the known phase diagrams, placing known stable and metastable structures on or near the convex hull of energy versus composition plots. The known stable and metastable structures also exhibit mechanical stability under static relaxation. Comparisons of the sequence of binary alloys Al-Cu, Al-Ni, and Al-Co, and comparisons of the ternary alloys Al-Co-Cu and Al-Co-Ni, accurately reflect the variations in phase diagrams among these compounds.

The range of applicability of the present Al-Co-Cu pair potentials extends up to a total transition-metal concentration of 50% provided the Co concentration is below 25%. The range of validity includes the composition of a decagonal quasicrystal phase. Even within this range, however, small errors are observed in the spurious appearance of a presumed metastable τ phase on the convex hull, and the calculated metastability of a known stable phase Al_7CoCu_2.

More serious are the difficulties at larger Co concentrations. Here, both the assumption of constant electron density and the neglect of many-body interactions limit the useful application of the zero-TM-concentration pair potentials. As previously found for $Al_{1-x}Co_x$, full volume- and concentration-dependent GPT pair potentials and/or corresponding three- and four-body Co potentials are needed to accurately address this regime.[16]

ACKNOWLEDGMENTS

M.W. acknowledges support by the National Science Foundation under Grant No. DMR-9732567. I.A. is supported by the Saudi Arabian government. The work of the JAM was performed under the auspices of the U.S. Department of Energy by the Lawrence Livermore National Laboratory under contract number W-7405-ENG-48.

[1] *Intermetallic Compounds: Principles and practice*, edited by J. H. Westbrook and R. L. Fleischer (Wiley, New York, 1995).

[2] *Emerging Engineering Materials*, edited by M. M. Schwartz (Technomic, Lancaster, PA, 1996).

[3] D. P. Shoemaker and C. B. Shoemaker, in *Introduction to Quasicrystals*, edited by M. V. Jaric (Academic, San Diego, 1988), p. 1.

[4] For reviews of topics in the field of quasicrystals, see *Quasicrystals: The State of the Art*, edited by D. P. DiVincenzo and P. J. Steinhardt (World Scientific, Singapore, 1991); C. Janot, *Quasicrystals: A Primer* (Oxford University, New York, 1992).

[5] J. Hafner, *From Hamiltonians to Phase Diagrams* (Springer-Verlag, Berlin, 1987).

[6] D. Pettifor, *Bonding and Structure of Molecules and Solids* (Clarendon Press, Oxford, 1995).

[7] *Ab initio* electronic-structure studies of Al-rich intermetallic systems include M. Windisch, M. Krajčí, and J. Hafner, J. Phys.: Condens. Matter **6**, 6977 (1994); G. Trambly de Laissardiere and T. Fujiwara, Phys. Rev. B **50**, 9843 (1994); G. Trambly de Laissardiere, D. Nguyen Manh, L. Magaud, J. P. Julien, F. Cyrot-Lackmann, and D. Mayou, *ibid.* **52**, 7920 (1995); R. F. Sabiryanov, S. K. Bose, and S. E. Burkov, J. Phys.: Condens. Matter **7**, 5437 (1995).

[8] M. Krajčí, J. Hafner, and M. Mihalkovič, Phys. Rev. B **56**, 3072 (1997).

[9] J. A. Moriarty and A. K. McMahan, Phys. Rev. Lett. **48**, 809 (1982); A. K. McMahan and J. A. Moriarty, Phys. Rev. B **27**, 3235 (1983).

[10] J. A. Moriarty, Phys. Rev. B **38**, 3199 (1988).

[11] M. Krajčí and J. Hafner, Phys. Rev. B **46**, 10669 (1992).

[12] M. Windisch, J. Hafner, M. Krajčí, and M. Mihalkovič, Phys. Rev. B **49**, 8701 (1994).

[13] R. Phillips, J. Zou, A. E. Carlsson, and M. Widom, Phys. Rev. B **49**, 9322 (1994).

[14] M. Mihalkovič, W.-J. Zhu, C. L. Henley, and R. Phillips, Phys. Rev. B **53**, 9021 (1996).

[15] J. A. Moriarty and M. Widom, Phys. Rev. B **56**, 7905 (1997).
[16] M. Widom and J. A. Moriarty, Phys. Rev. B **58**, 8967 (1998).
[17] B. Grushko, Phase Transit. **44**, 99 (1993).
[18] B. Grushko, in *Aperiodic '94*, edited by G. Chapuis and W. Paciorek (World Scientific, Singapore, 1995).
[19] T. Gödecke, M. Scheffer, R. Lück, S. Ritsch, and C. Beeli, Z. Metallkd. **89**, 687 (1998).
[20] L. X. He, Y. K. Wu, and K. H. Kuo, J. Mater. Sci. Lett. **7**, 1284 (1988); A.-P. Tsai, A. Inoue, and T. Masumoto, Mater. Trans., JIM **30**, 300 (1989).
[21] T. Gödecke, M. Scheffer, R. Lück, S. Ritsch, and C. Beeli, Z. Metallkd. **88**, 687 (1997).
[22] J. A. Moriarty, Phys. Rev. B **49**, 12 431 (1994).
[23] M. Widom and E. Cockayne, Physica A **232**, 713 (1996).
[24] J. Grin, U. Burkhardt, M. Ellner, and K. Peters, J. Alloys Compd. **206**, 243 (1994).
[25] C. Freiburg, B. Grushko, R. Wittenberg, and W. Reichert, Mater. Sci. Forum **228-231**, 583 (1996).
[26] J. L. Murray, Int. Met. Rev. **30**, 211 (1985).
[27] M. El-Boragy, R. Szepan and K. Schubert, J. Less-Common Met. **29**, 133 (1972).
[28] G. D. Preston, Philos. Mag. **12**, 980 (1931).
[29] P. Villars and L. D. Calvert, *Pearson's Handbook of Crystallographic Data for Intermetallic Phases* (American Society for Metals, Materials Park, OH, 1991).
[30] B. Zhang, V. Gramlich, and W. Steurer, Z. Kristallogr. **210**, 498 (1995).
[31] K. Chattopadhyay, S. Lele, N. Thangaraj, and S. Ranganathan, Acta Metall. **35**, 727 (1987).
[32] R. C. Hudd and W. H. Taylor, Acta Crystallogr. **15**, 441 (1962).
[33] S. S. Lu and T. Chang, Sci. Sin. **13**, 150 (1957); G. van Tendeloo, C. van Heurck, and S. Amelinckx, Solid State Commun. **71**, 705 (1989).
[34] G. V. S. Sastry, K. K. Bariar, K. Chattopadhyay, and P. Ramachandrarao, Z. Metallkd. **71**, 756 (1980).
[35] L. X. He, X. Z. Li, Z. Zhang, and K. H. Kuo, J. Mater. Sci. Lett. **7**, 1284 (1988).
[36] M. G. Bown and P. J. Brown, Acta Crystallogr. **9**, 911 (1956).
[37] N. Ridley, J. Inst. Met. **94**, 255 (1966).
[38] E. Cockayne and M. Widom, Phys. Rev. Lett. **81**, 598 (1998).
[39] G. V. Raynor, Prog. Met. Phys. **1**, 1 (1949).
[40] B. Grushko and K. Urban, Philos. Mag. B **70**, 1063 (1994).
[41] C. Freiburg and B. Grushko, Z. Kristallogr. **209**, 49 (1994).
[42] E. Cockayne and M. Widom, Philos. Mag. A **77**, 593 (1998).
[43] M. Mihalkovič, F. Dugain, and J. B. Suck, J. Non-Cryst. Solids **205-207**, 701 (1996).
[44] M. Widom, I. Al-Lehyani, Y. Wang, and E. Cockayne, Mater. Sci. Eng. A (to be published).
[45] I. Al-Lehyani, N. Moghadam, J. A. Moriarty, Y. Wang, and M. Widom (unpublished).
[46] J. A. Moriarty, Phys. Rev. B **42**, 1609 (1990).
[47] We are indebted to Marek Mihalkovic for developing the computer program used in this simulation.